PLC Channel: Impulsive Noise Modelling and Its Performance Evaluation Under Different Array Coding Schemes

Nikoleta Andreadou, *Member, IEEE*, and Fotini-Niovi Pavlidou, *Senior Member, IEEE*

***Abstract*—Power-line communications (PLC) is a field that has raised a lot of research in the past years. In this paper, we introduce array codes into the PLC environment and we study the channel's performance. In particular, generalized array codes (GAC), as well as row and column array codes (RAC) are applied. We examine their performance by obtaining three different code rates from each category. Therefore, the (8, 4, 4), (12, 7, 4) and (16, 11, 4) GAC codes as well as the (9, 4, 4), (12, 6, 4), and (15, 8, 4) RAC codes are used, meaning that we obtain code rates of (1/2), (7/12), (11/16), and (4/9), (6/12), (8/15) respectively. In addition, for reasons of completeness, convolutional codes are also being applied under the same channel conditions. Moreover, we suggest a hybrid coding technique, which combines the (8, 4, 4) GAC and the (15, 8, 4) RAC code in order to meet the requirements of the PLC time-varying channel and improve its performance. Concerning the system's design, we take into consideration Zimmermann's model for the PLC channel. We apply Middleton's model for the channel's background and impulsive noise, while we also introduce a novel way of estimating the system's impulsive noise. Finally, the well-known transmission technique of orthogonal frequency-division multiplexing is used. The channel's performance is evaluated in terms of the bit-error rate for different E_b/N_0 values via computer simulations.**

***Index Terms*—Generalized array codes (GACs), impulsive noise, power-line communications (PLC), row column codes (RAC codes).**

I. Introduction

THE increasing demand for data and voice transmission over the past years, has led to a "spectrum drought," implying that alternative ways of communication are fundamental. Power-line communications (PLC) constitutes an innovative manner of information exchange. They imply transmission of the telecommunication signal through the public power network, which makes this new technology appealing since the existing infrastructure is utilized and there is no need for new wires. On the other hand, there are several drawbacks concerning this technology, which need to be overcome for better system performance. One main drawback is that the network was not originally designed for high-frequency signals; therefore, it introduces great variance to different signal components. Furthermore, due to the changing load on the power network, impulsive noise is added to the communication signal, which makes it even harder for the data to be recovered at the receiver.

In order to simulate a PLC system, it is essential that the channel characteristics are modelled. In the literature, there are several channel models available. One of the first channel models was introduced by Hensen and Schulz, which was a simple model implying that the attenuation increased with frequency [1]. "Philipps" model was introduced next, and took into consideration the multipath effect of the transmission through the power lines' network [2]. This model is applied in the time domain, since it entails each path's delay in time. A frequency-domain channel model was introduced by Zimmermann and Dostert, [3]. This model not only estimates the delay that each path encloses, but also the attenuation that it undergoes due to the wire's length. Therefore, it is considered to be a more in-depth channel model. Moreover, Banwell and Galli proposed a channel model based on the multiconductor transmission-line theory, where, the power line can be represented by an equivalent circuit [4], [5]. Finally, there are several channel models introduced by various researchers which are based on measurements [6]–[8]. In this paper, Zimmermann's model is used, because it is easy to apply. It takes many parameters into account and is used a lot in the literature as a reference channel model.

It should be also mentioned that the telecommunication signal suffers deterioration due to the noise added by the channel. The noise can be divided into two categories: 1) background noise and 2) impulsive noise. Similar to the occasion of channel models, there are several noise models available in the literature for background and impulsive noise. The majority of these models are based on measurements. Some examples of such models can be found in [9]–[15]. One popular noise model used by a lot of researchers in the literature is Middleton's model [16], which we also take into account in our study. According to this model, the total noise consists of two parts, describing the background and impulsive noise, respectively. However, according to [15], it does not describe impulsive noise in the most accurate way. Therefore, we introduce a new way of estimating the impulsive noise by exploiting the noise bursts' properties. According to these properties, noise bursts are Poisson distributed with an impulse arrival rate of

$$0 \leq \lambda \leq 5 * 10^{(-3)} \quad (1)$$

Manuscript received February 04, 2008; revised March 24, 2008. First published February 13, 2009; current version published March 25, 2009. This work was supported by the Greek General Secretariat for Research and Technology under Grant "PENED 2003." Paper no. TPWRD-00070-2008.

The authors are with the Aristotle University of Thessaloniki, Thessaloniki 54124, Greece (e-mail: nandread@auth.gr).

Digital Object Identifier 10.1109/TPWRD.2008.2002958

whereas their duration takes no longer than 0.1 ms [9]. Keeping these properties in mind, the impulse noise's effect on our data can be easily derived, as explained further in the next section.

In order for a complete PLC system to be simulated, coding and modulation techniques should be implemented. In this paper, we introduce array codes and specifically generalized array codes (GACs) and row and column array codes (RACs) as the system's coding scheme. These codes are mainly examined by Soyjaudah, [17]–[19] and Feng [20], [21]. However, never before have they been used in a PLC environment. Thus, it is practical to study their effectiveness in a PLC channel.

The rest of this paper is arranged as follows. Section II describes the PLC channel model as well as the applied noise models. In Section III, RAC and GAC codes are described, the coding and decoding techniques taken into consideration for the system's design. In Section IV, the system's performance for the various coding schemes is displayed in terms of BER versus different $\mathrm{E_b/N_0}$ values. In Section V, a hybrid coding technique for the time-varying channel is proposed. Finally, the conclusions are drawn in Section VI.

II. Channel and Noise Models

A. PLC Channel Model

As was mentioned before in this paper, we take Zimmermann's channel model [3] into consideration; since it is easily applicable, it takes useful parameters into account and it is used by many investigators. It is a frequency channel model and it involves the attenuation introduced to the communications signal by cable losses as well as the multipath effect. According to the latter phenomenon, the signal reaching the receiver consists of several components, which have travelled through different paths. Only the N dominant paths are used in the model. The signal components undergo a different amount of delay since the route they follow is not the same. Furthermore, a weighting factor g (less than or equal to 1) is used for each path, demonstrating the reflections that occur along with it. The model's frequency response is given by the following equation:

$$H(f)=\sum_{i=1}^{N}\underbrace{g_i}_{\text{weighting factor}}\cdot\underbrace{e^{-(\alpha_0+\alpha_1\cdot f^k)\cdot d_i}}_{\text{attenuation portion}}\cdot\underbrace{e^{-j2\pi f\cdot(d_i/\upsilon_p)}}_{\text{delayportion}}. \tag{2}$$

The factor d_i/u_p stands for the time delay τ_{i} of each path, where τ_i is

$$\tau_i=\frac{d_i\cdot\sqrt{\varepsilon_r}}{c_0}=\frac{d_i}{\upsilon_p} \tag{3}$$

where d_i is the length of the path, ε_r is the dielectric constant of the insulating material, and c_0 is the speed of light.

The attenuation portion in the equation stands for the signal's deterioration due to cable losses, whereas the parameters α_0, α_1 and k are based on cable parameters, depending on geometric dimensions and material properties. Both the attenuation and delay portion depend on the frequency f.

The values of the parameters shown in (1), in addition to the number of the dominant paths used for the calculations of the channel model, can be found in [3].

B. Noise Models

In a power-line channel, noise can be divided into two categories: 1) background and 2) impulsive noise. Background noise experiences small deviations with time, whereas impulsive noise is characterized by rapidly modified amplitude, which is mainly caused by the varying amount of appliances switched on the power network.

Due to its unpredictable nature, noise is harder to model. Basically, noise models are derived by measurements. In the literature, frequency- [9]–[12] and time-domain [13], [14] models can be found, according to the method used for their development, which refers to background as well as impulsive noise.

It should be mentioned here that a noise model used a lot in the literature [22], [23] for PLC channels is Middleton's class A model [16]. It consists of background and impulsive noise, and it is used to represent the noise on power-line channels. According to the model, the probability density function of the noise amplitude v is given by the subsequent equation

$$p(v)=\sum_{k=0}^{\infty}\frac{e^{-A}\cdot A^k}{k!}\cdot\frac{1}{\sqrt{2\pi}\cdot\sigma_k}\cdot\exp\left(\frac{-v^2}{2\cdot\sigma_k^2}\right) \tag{4}$$

where

$$\sigma_k^2=P\cdot\frac{(k/A)+\Gamma}{1+\Gamma}$$
$$P=\sigma_G^2+\sigma_I^2,\ \text{total noise power}$$
$$\sigma_G^2\rightarrow\ \text{Gaussian noise power}$$
$$\sigma_I^2\rightarrow\ \text{Impulsive noise power}$$
$$\Gamma=\sigma_G^2/\sigma_I^2$$
$$\mathrm{A}\rightarrow\ \text{Impulsive index}.$$

It can be clearly assumed that the impulsive noise follows Poisson distribution. According to [16], a noise sample can be given by the equation

$$n=x_G+\sqrt{K_m}\cdot y \tag{5}$$

where

$x_G\rightarrow$ is the white Gaussian background noise sequence with zero mean and variance σ_G^2;

$y\rightarrow$ is the white Gaussian sequence with zero mean and variance σ_I^2/A;

$K_m\rightarrow$ is the Poisson distributed sequence whose pdf is characterized by the impulsive index A.

Its concept is that impulsive noise contributes to the overall noise sample according to a Poisson-distributed random sequence. In our investigation, Middleton's class A noise model is being used to model PLC channel noise, with parameters $\mathrm{A}=0.1$ and $\Gamma=0.1$, implying that the impulsive noise is ten times stronger than the background noise.

However, according to [15], Middleton's class A model may not be the most suitable candidate to describe impulsive noise in the PLC environment since it is originally designed for man-made interference. Therefore, we introduce a new way of modeling the impulsive noise in the power network, by taking the noise bursts' properties into account, and compare the results with those obtained when Middleton's model is applied in the system.

TABLE I
PARAMETERS OF IMPULSIVE NOISE MODEL

	Minimum value	Maximum value	Mean value
Interarrival time	0 sec	0.005 sec	0.0025 sec
Impulse noise duration	0.1 ms		

TABLE II
VALUES FOR IMPULSE NOISE DURATION

Interarrival time			Impulse noise duration
Minimum value	Maximum value	Mean value	
0 sec	0.005 sec	0.0025 sec	0.01 ms
			1 ms

TABLE III
VALUES FOR INTERARRIVAL TIME

Interarrival Time			Impulse noise Duration
Minimum Value	Maximum Value	Mean Value	
0 sec	0.001 sec	0.0005 sec	0.1 ms
0 sec	0.01 sec	0.005	

Our concept is based on the fact that impulsive noise can be expressed in terms of bursts that damage our data when they occur. As a result, if no burst appears at a particular moment, our data carriers will not be influenced by this kind of noise. Since we apply orthogonal frequency-division multiplexing (OFDM) transmission, our data are transferred in terms of blocks, each block representing an OFDM symbol. Therefore, all we need to estimate is which blocks are influenced, and at what extent by the impulse bursts. This is directly related to the noise bursts' properties, such as their interarrival rate and the distribution they follow. According to [4], noise bursts last no longer than 0.1 ms and they are characterized by a Poisson distribution with an impulse arrival rate of $0 \leq \lambda \leq (5 * 10^{-3})$.

Statistics and probability theory indicate that since the noise bursts are Poisson distributed, the interval between them is described by an exponential distribution. Keeping these properties in mind, we created a computer program which produces Poisson-distributed impulse bursts and subsequently estimates the effect they have on the OFDM symbols that are transferred under the existence of noise bursts.

Similar to the case of Middleton's class A model, we consider impulsive noise to be ten times more powerful than background noise, which is evaluated the same way as was done previously. As a result, by following these logical steps, we created a simple and practical model adding impulsive noise to our system. The parameters used are illustrated in Table I.

The interarrival time is produced randomly by the computer program. For reasons of completeness, we also check how these parameters affect the system's performance. Therefore, we alter their values and compare the results in terms of the bit-error rate (BER) obtained. At first, the interarrival time is kept stable while different values are assigned to the impulse noise duration in order to test its effect on the system's performance. On the other hand, we examine the influence on the resulting BER by the bursts' rate, by altering the interarrival time, while the impulse noise duration has a stable value. Tables II and III illustrate the aforementioned information.

III. ENCODING AND DECODING TECHNIQUES

In this study, we implement GACs and RACs for coding and decoding techniques, since, to the best of our knowledge, never before have they been introduced to a PLC environment. In general, array codes have a simple structure of two or more dimensions and are built from component codes [17]. Although RAC and GAC codes have many similar features, they also have vital differences, which are pointed out in this section.

A. Encoding Procedure of RAC Codes

These codes can be rectangular or square in shape. The information bits are organized in such a way so as to form an array of k_1 rows and k_2 columns. Subsequently, an array of n_1 rows and n_2 columns is derived by performing the single parity check operation on rows and columns, with $\mathrm{n}_1 = \mathrm{k}_1 + 1$ and $n_2 = k_2 + 1$. The resulting code is an (n, k, 4) RAC code with $n = n_1 * n_2, k = k_1 * k_2$, whereas it has the capacity of correcting up to four errors [17].

Since the codes used in our simulations are the (9, 4, 4), the (12, 6, 4), and the (15, 8, 4) RAC codes, we present their structures in terms of matrices C_1,, C_2, and C_3, given by (6)–(8), respectively

$$C_1 = \begin{bmatrix} x_1 & x_2 & p_1 \\ x_3 & x_4 & p_2 \\ p_3 & p_4 & p_5 \end{bmatrix} \tag{6}$$

where $\mathrm{x_i}, \mathrm{i} = 1, \ldots 4$ are the information bits and $\mathrm{p_j}, \mathrm{j} = 1, \ldots 5$ are the parity bits

$$p_1 = x_1 \oplus x_2, \quad p_2 = x_3 \oplus x_4$$
$$p_3 = x_1 \oplus x_3, \quad p_4 = x_2 \oplus x_4$$

and $p_5 = p_1 \oplus p_2$.

With this type of coding scheme, it is easily figured out that we obtain a code rate of $\mathrm{r}_1 = \mathrm{k}/\mathrm{n} = 4/9$, since we obtain nine coded bits for every four data bits

$$C_2 = \begin{bmatrix} x_1 & x_2 & x_3 & p_1 \\ x_4 & x_5 & x_6 & p_2 \\ p_3 & p_4 & p_5 & p_6 \end{bmatrix} \tag{7}$$

where $x_i, i = 1, \ldots 6$ are the information bits and $p_j, j = 1, \ldots 6$ are the parity bits

$$p_1 = x_1 \oplus x_2 \oplus x_3, p_2 = x_4 \oplus x_5 \oplus x_6, p_3 = x_1 \oplus x_4$$

$p_4 = x_2 \oplus x_5, p_5 = x_3 \oplus x_6$ and $p_6 = p_1 \oplus p_2$. Similar to the case of (9, 4, 4) RAC code, the code rate for (12, 6, 4) RAC code is $r_2 = 6/12$

$$C_3 = \begin{bmatrix} x_1 & x_2 & x_3 & x_4 & p_1 \\ x_5 & x_6 & x_7 & x_8 & p_2 \\ p_3 & p_4 & p_5 & p_6 & p_7 \end{bmatrix} \tag{8}$$

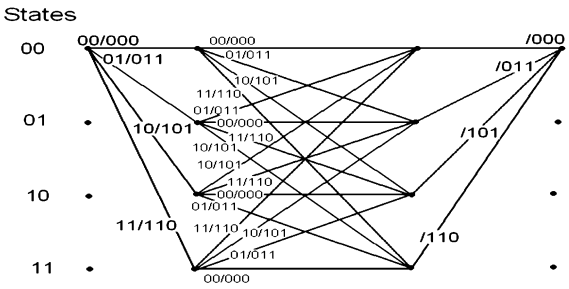

Fig. 1. Trellis diagram of (9, 4, 4) the RAC code with $N_s = 4$ 4 and $N_c = 4$.

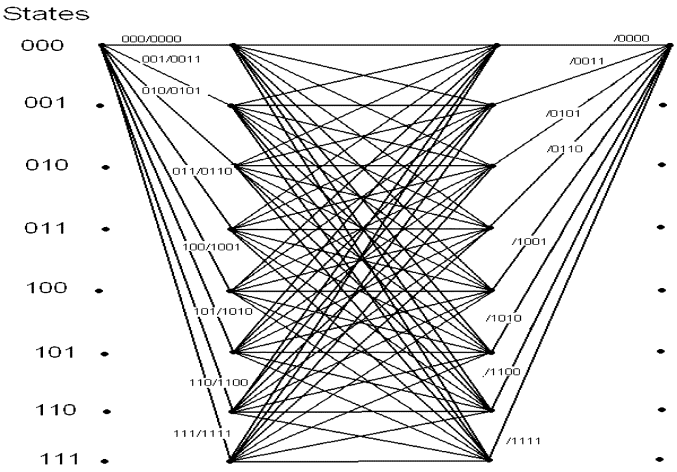

Fig. 2. Trellis diagram of (12, 6, 4) RAC code with $\mathrm{N_s} = 8$ and $\mathrm{N_c} = 4$.

where $x_i, i = 1, \ldots 8$ are the information bits and $p_j, j = 1, \ldots 7$ are the parity bits, derived in a corresponding way as shown before. The resulting code rate is $r_3 = 8/15$.

It should be also mentioned at this point that the necessary modulation scheme depends on the encoding procedure and more precisely on the information bits per row. The reason for this is because the bits entailed in each row are reassigned to one modulation symbol, thus determining the modulation scheme.

It is noticeable that the potential symbols for transmission for the (9, 4, 4) RAC code are up to four, whereas in the cases of the (12, 6, 4) and the (15, 8, 4) RAC codes, they are no more than 8 and 16, respectively. Therefore, the corresponding modulation schemes used for our system's design are the quadrature phase-shift keying (QPSK), the 8 PSK, and the 16 PSK.

B. Decoding Procedure of RAC Codes

The decoding procedure of RAC codes is performed easily if we take their corresponding trellis diagrams into account. This process, in order to construct the trellis diagram, is explained in [17] and is shown in the Appendix.

The trellis diagrams for the codes of our interest, the (9, 4, 4), the (12, 6, 4), and the (15, 8, 4) RAC code are demonstrated in Figs. 1–3, respectively.

In Fig. 1, we display the input/output vectors for the decoder. For reasons of simplicity and clarification, the majority of the input and output vectors in Figs. 2 and 3 have been omitted.

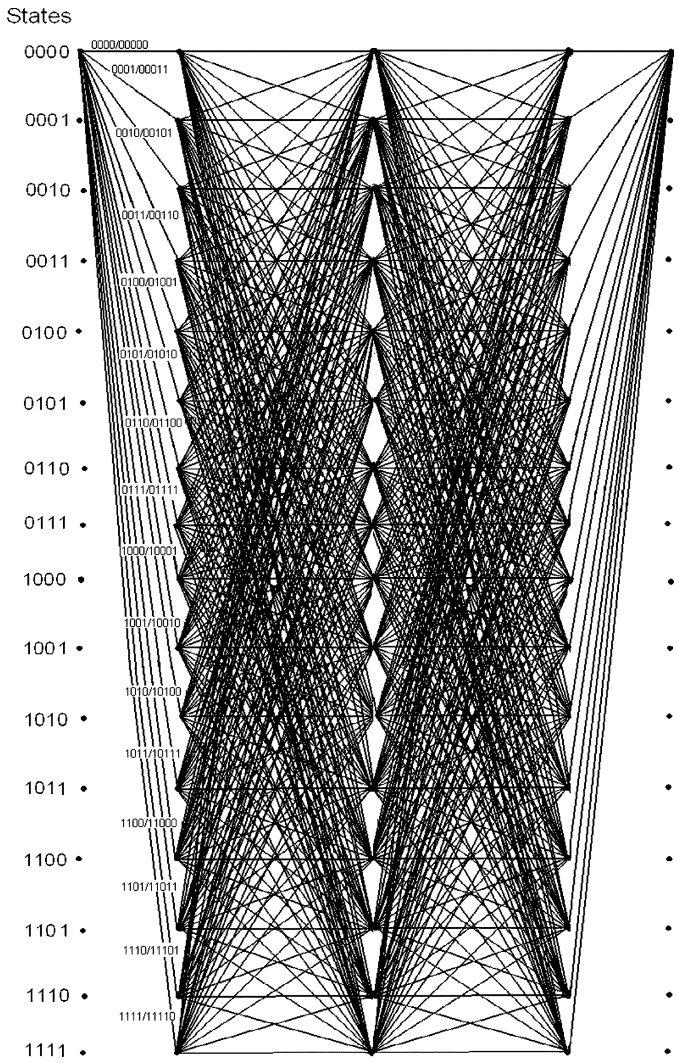

Fig. 3. Trellis diagram of (15, 8, 4) RAC code with $\mathrm{N_s} = 16$ and $\mathrm{N_c} = 5$.

C. Encoding Procedure of GAC Codes

The concept of a generalized $(n, k, d_{\min})$ array code is similar to that of RAC codes; however, the first scheme may entail row and column subcodes with different numbers of information and parity check bits. The total number of information bits is

$$k = k_1 + k_2 + \cdots + k_{n_2} \tag{9}$$

where $k_p, p = 1, \ldots, n_2$ is the number of information bits in the pth row. On the other hand, the total number of coded bits is $n = n_1 * n_2$, with n_1 and n_2 being the number of rows and columns, respectively.

The procedure that was followed in order to construct a generalized array code (n_0, k_0, d_0) is found in [19] and shown in the Appendix.

We implement this algorithm for the construction of the (8, 4, 4), the (12, 7, 4), and the (16, 11, 4) GAC code. For the first case, we obtain

$$C_{8,4,4} = \begin{bmatrix} x_1 & x_4 \oplus p_1 \\ x_2 & x_4 \oplus p_2 \\ x_3 & x_4 \oplus p_3 \\ p_4 & x_4 \oplus p_4 \end{bmatrix} \tag{10}$$

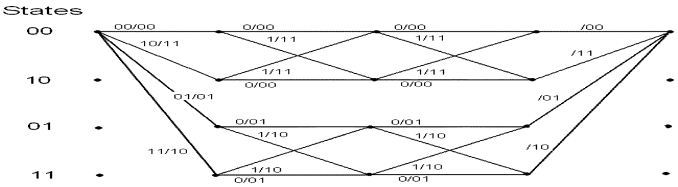

Fig. 4. Trellis diagram of (8, 4, 4) GAC code with $N_s = 4$ and $N_c = 5$.

where $x_i, i = 1, \ldots 4$ are the information bits, $p_j, j = 1, \ldots 4$ are the parity bits, and $p_i = x_i, i = 1, 2, 3$ and $p_4 = x_1 \oplus x_2 \oplus x_3$. The code rate is 4/8, since there are eight coded bits for every four information bits.

For the (12, 7, 4) GAC code, we obtain

$$C_{12,7,4} = \begin{bmatrix} x_1 & x_4 & p_1 \oplus x_7 \\ x_2 & x_5 & p_2 \oplus x_7 \\ x_3 & x_6 & p_3 \oplus x_7 \\ p_4 & p_5 & p_6 \oplus x_7 \end{bmatrix} \tag{11}$$

where $x_i, i = 1, \ldots 7$ are the information bits, and $p_j, j = 1, \ldots 6$ are the parity bits, $p_1 = x_1 \oplus x_4, p_2 = x_2 \oplus x_5, p_3 = x_3 \oplus x_6, p_4 = x_1 \oplus x_2 \oplus x_3, p_5 = x_4 \oplus x_5 \oplus x_6$. The code rate achieved for the (12, 7, 4) GAC code is 7/12.

Finally, for the (16, 11, 4) GAC code, we obtain

$$C_{16,11,4} = \begin{bmatrix} x_1 & x_2 & x_3 & p_1 \oplus x_{10} \\ x_4 & x_5 & x_6 & p_2 \oplus x_{10} \\ x_7 & x_8 & x_9 & p_3 \oplus x_{10} \\ p_4 \oplus x_{11} & p_5 \oplus x_{11} & p_6 \oplus x_{11} & p_7 \oplus x_{10} \oplus x_{11} \end{bmatrix} \tag{12}$$

where $x_i, p_j, i = 1, \ldots 11$ and $j = 1, \ldots 7$ are the information and parity bits, respectively, with $p_1 = x_1 \oplus x_2 \oplus x_3, p_2 = x_4 \oplus x_5 \oplus x_6, p_3 = x_7 \oplus x_8 \oplus x_9, p_4 = x_1 \oplus x_4 \oplus x_7, p_5 = x_2 \oplus x_5 \oplus x_8, p_6 = x_3 \oplus x_6 \oplus x_9$, and $p_7 = p_4 \oplus p_5 \oplus p_6$. As we notice, the code rate is 11/16.

Similar to RAC codes, each row of the matrix is transferred to one modulation symbol; therefore, the required modulation scheme differs for each GAC code and is directly related to the number of information bits per row.

As we can observe, the potential transmitted symbols do not exceed number four concerning the (8, 4, 4) GAC code and number 8 and 16 regarding the (12, 7, 4) and the (16, 11, 4) GAC code. Thus, the modulation schemes utilized are the QPSK, the 8 PSK and the 16 PSK correspondingly.

D. Decoding Procedure of GAC Codes

Likewise, in the case of RAC codes, the decoding of GAC codes is easily carried out via the trellis diagram. The steps in order to accomplish its design [19] are shown in the Appendix.

In Figs. 4–6, we display the trellis diagrams of the examined (8, 4, 4), (12, 7, 4), and (16, 11, 4) GAC codes. In Fig. 6, most of the input and output vectors have been omitted due to clarification reasons.

IV. Coding Schemes Performance via Simulations

In this section, we show the BER performance of the examined coding schemes in a PLC environment. As explained in the previous section, we apply two different techniques to model the system's impulsive noise and we present the BER results for both approaches. The simulations were not an easy task to perform since a frequency channel model was utilized, while the OFDM transmission technique implies that a cyclic extension of the symbol is necessary in the time domain. Therefore, careful operations of the fast Fourier transform (FFT) and inverse fast Fourier transform (IFFT) functions were required during the signal's transmission and reception, so as to transfer our data from the frequency to time domain and vice versa. Due to these transformations and the numerous components that the systems consist of, the total simulation time was large. Consequently, there had to be a tradeoff between the number of transmitted data blocks and the minimum possible BER value that the results approach. So the number of transmitted data blocks was set to 1000 in each case, whereas each block was transmitted over an OFDM symbol consisting of 256 subcarriers. The number of total data bits for the different cases of each coding technique depended on the modulation scheme required. Since the modulation scheme is defined by the particular code used, the results are grouped into three categories according to which modulation techniques are applied (QPSK, 8 PSK, or 16 PSK), so that a better results' comparison is obtained. For reasons of completeness, convolutional codes modulated with QPSK, 8 PSK and 16 PSK are also examined; so their performance is compared to the one obtained from GAC and RAC codes.

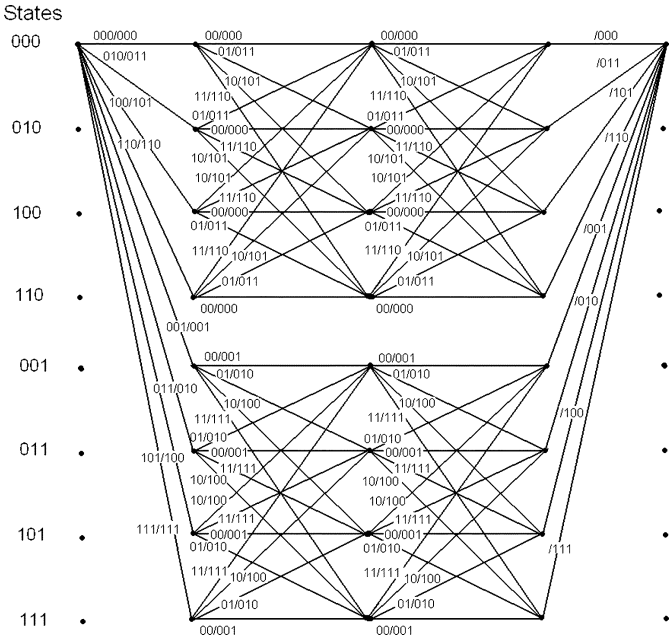

Fig. 5. Trellis diagram of (12, 7, 4) GAC code with $N_s = 8$ and $N_c = 5$.

In Figs. 7–9, we illustrate the system's performance in terms of BER versus the $\mathrm{E_b/N_0}$ value, provided that Middleton's noise model is utilized. Depending on the coding scheme examined, we obtain nine comparable yet different curves.

It is clearly noticeable that GAC codes show better performance than RAC codes throughout the whole $\mathrm{E_b/N_0}$ range, implying a stronger coding scheme. In Fig. 9, it is clearly observed that convolutional codes are inferior to RAC and GAC coding techniques, which becomes more obvious for higher $\mathrm{E_b/N_0}$

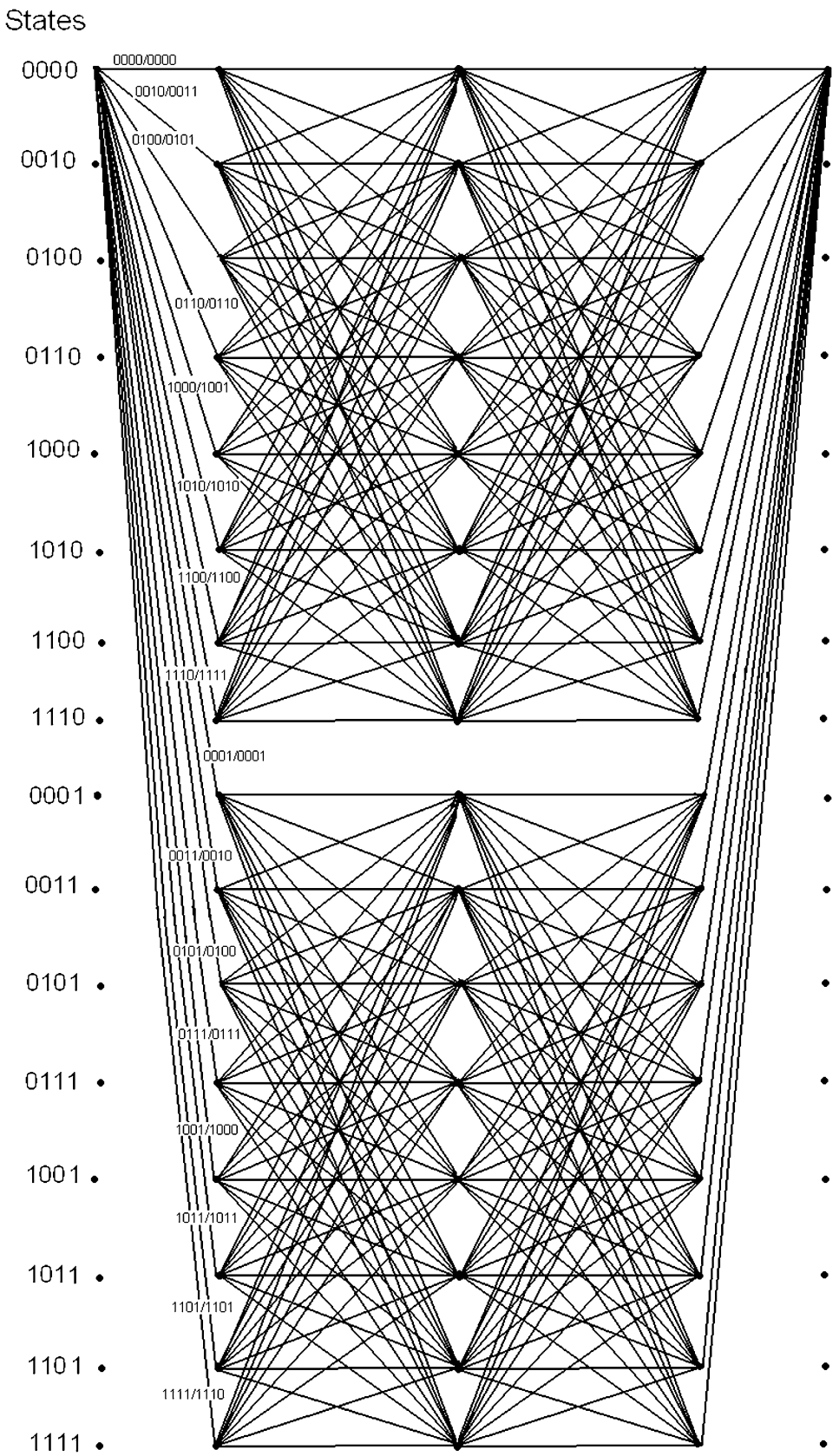

Fig. 6. Trellis diagram of (16, 11, 4) GAC code with $\mathrm{N_s} = 16$ and $\mathrm{N_c} = 5$.

values. The case is more or less the same regarding the codes requiring a QPSK or an 8PSK modulation scheme. However, as illustrated in Figs. 7 and 8, RAC codes' performance resembles the one of the convolutional code, with the latter being slightly inferior for higher $\mathrm{E_b}/\mathrm{N_0}$ values. By taking a closer look at Figs. 7–9, we observe that the modulation parameters also play

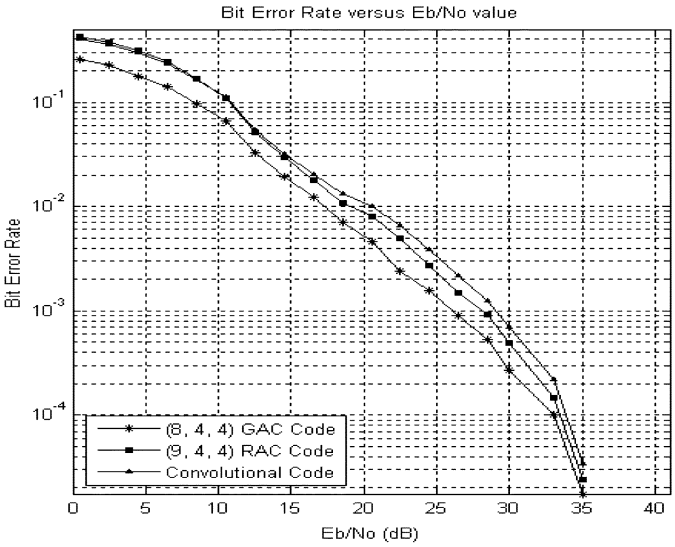

Fig. 7. BER versus $\mathrm{E_b/N_0}$ for QPSK modulation and Middleton's noise model.

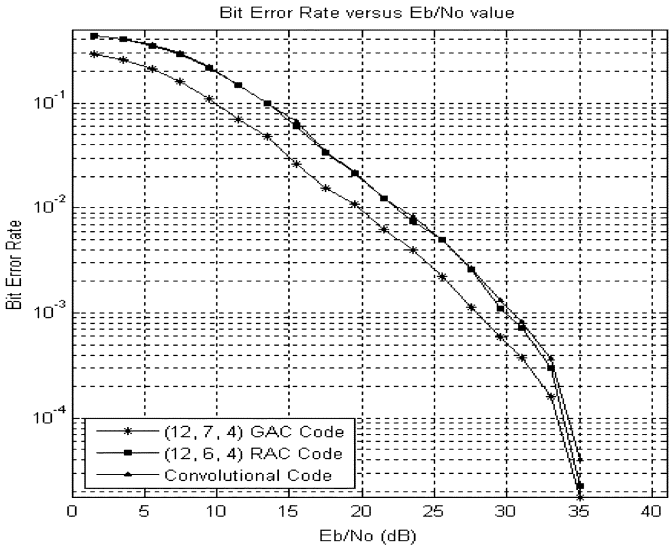

Fig. 8. BER versus $\mathrm{E_b/N_0}$ for 8PSK modulation and Middleton's noise model.

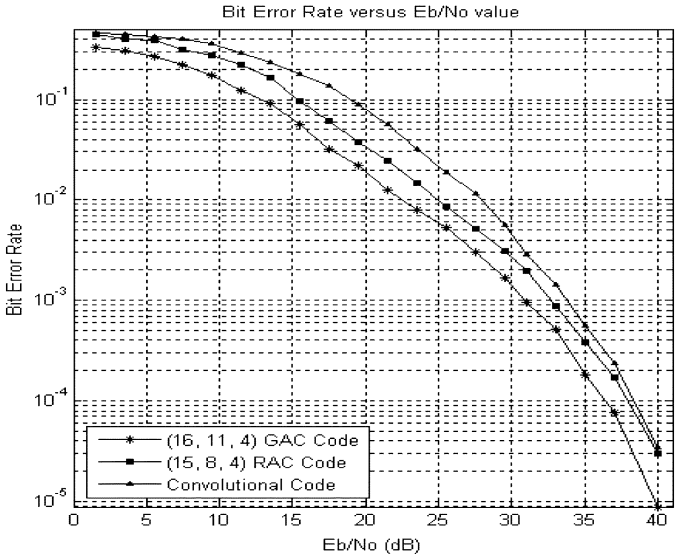

Fig. 9. BER versus $\mathrm{E_b/N_0}$ for 16PSK modulation and Middleton's noise model.

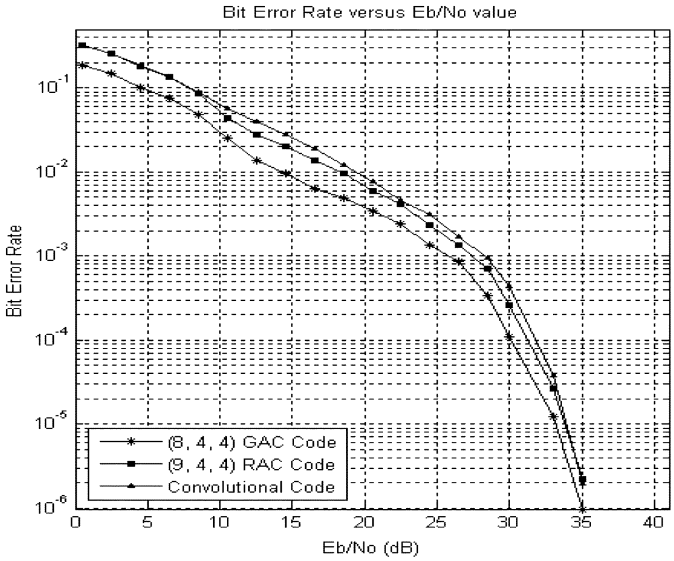

Fig. 10. Bit-error rate versus $\mathrm{E_b/N_0}$ for QPSK modulation and the proposed impulsive noise model.

an important role in determining the simulation results, since the QPSK-modulated data seem to reach the receiver with fewer errors. Therefore, as it is obvious from Fig. 9, we obtained results for higher $\mathrm{E_b/N_0}$ values in order to achieve the desired BER performance. However, applying 8PSK or 16PSK modulation implies better bandwidth exploitation; therefore, the selection of the modulation and coding scheme depends on the system's demands. Moreover, it should be also mentioned here that all curves follow the same trend, meaning that when the $\mathrm{E_b/N_0}$ value increases, the codes' performance improves. This denotes that all coding schemes respond in a comparable way under the same channel and noise conditions.

In Figs. 10–12, we demonstrate the system's performance when the proposed modified impulsive noise model is applied. The conclusions are more or less alike as before. Again, the GAC coding technique shows a greater tolerance against errors compared to the RAC coding technique. Convolutional codes seem to be slightly inferior to RAC codes in Figs. 10 and 11, whereas in Fig. 12, the latter codes clearly show better performance. All of the curves experience the same inclination throughout the whole $\mathrm{E_b/N_0}$ range, indicating that the influence made by the channel and noise conditions is of the same quality for all coding methods. Similar to the occasion of Middleton's noise model, when a higher modulation order is required by a coding technique, an inferior system's performance is obtained. This occurs since a greater modulation order indicates that more symbols are available at the receiver's demodulating process and the possibility of an error is thus larger.

After a thorough observation of the six figures, it can be concluded that the proposed impulsive noise model results in better BER values than the Middleton's noise model concerning the equivalent curves. However, the second scheme seems to perform better for higher $\mathrm{E_b/N_0}$ values.

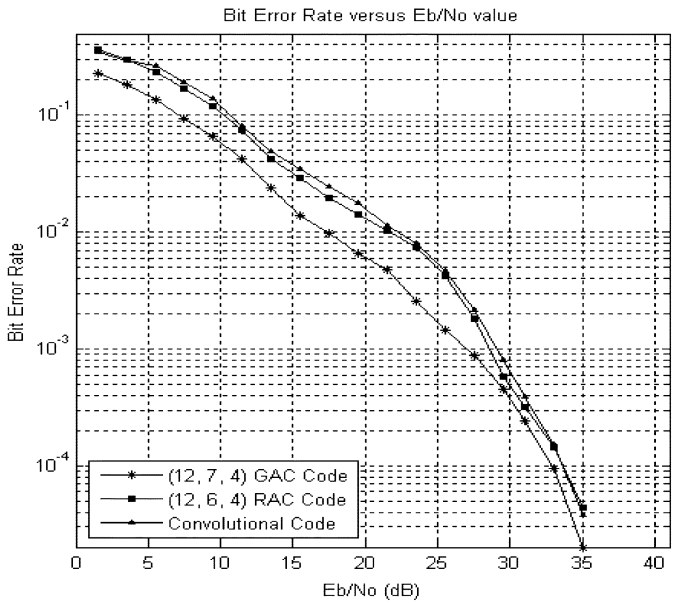

Fig. 11. Bit-error rate versus $\mathrm{E_b}/\mathrm{N_0}$ for 8PSK modulation and the proposed impulsive noise model.

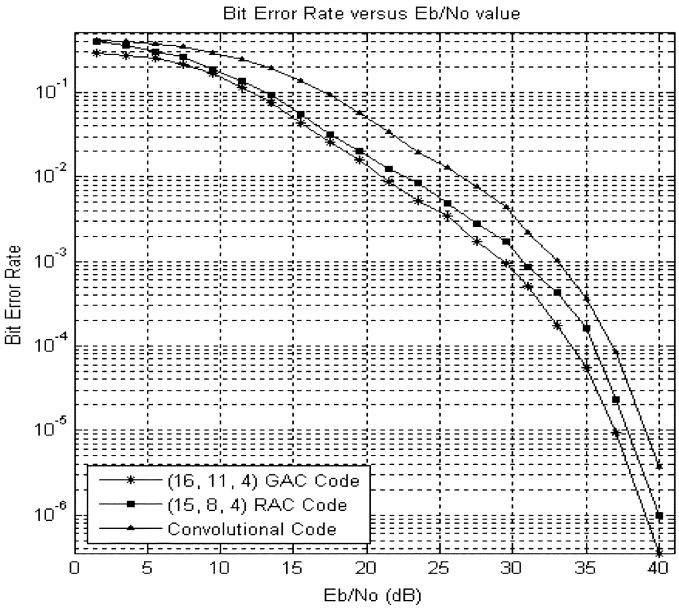

Fig. 12. BER versus $\mathrm{E_b}/\mathrm{N_0}$ for 16PSK modulation and the proposed impulsive noise model.

As has been mentioned in a previous section, the proposed impulsive noise model is also analyzed regarding its parameters. In particular, the effect of the impulse bursts' duration and their interarrival time are studied. Fig. 13 shows how different values of the former parameter impinge on the system's performance, while the latter one remains constant ($2.5 * 10^{-3}$ as a mean value). On the other hand, in Fig. 14, the impulse noise duration is stable (0.1 ms), whereas different values of the bursts' interarrival time are used to illustrate the effect on the system's performance.

It can be easily concluded from Figs. 13 and 14, that all of the encoding schemes behave in a similar way under the same channel conditions.

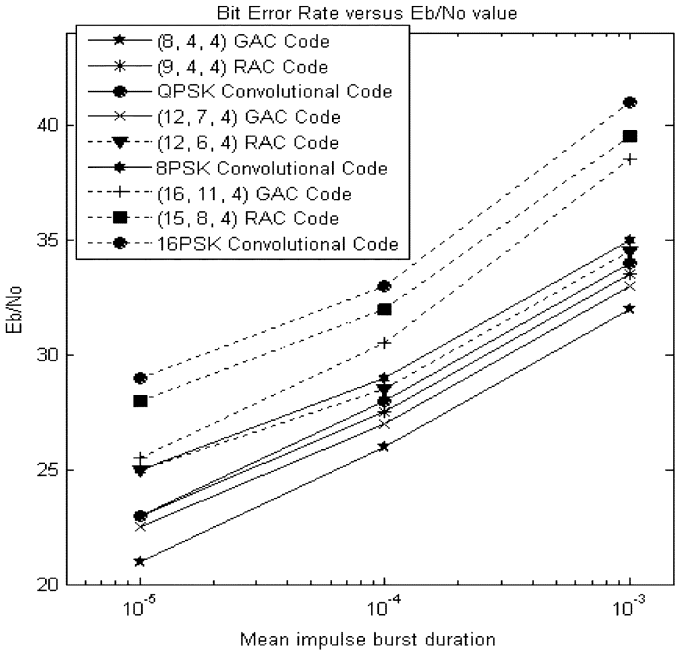

Fig. 13. $\mathrm{E_b}/\mathrm{N_0}$ at $\mathrm{BER} = 10^{-3}$ versus different values of impulse noise duration for all of the examined coding schemes and the proposed impulsive noise model.

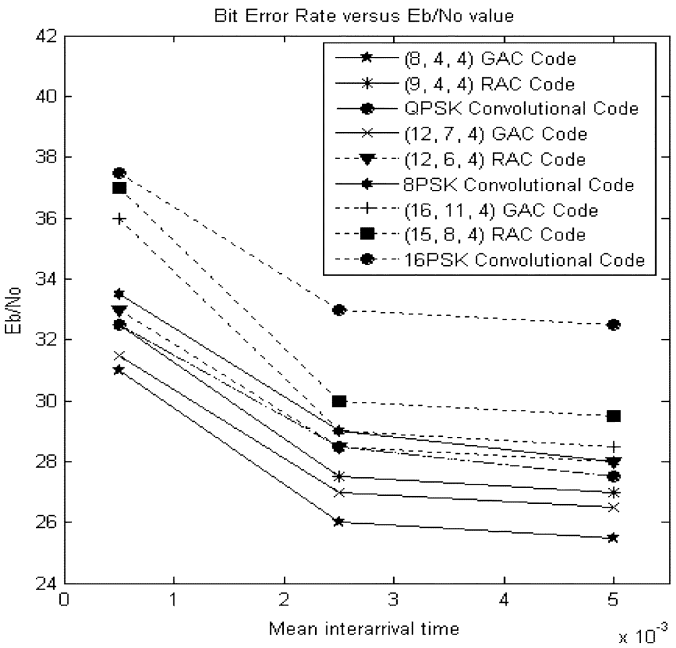

Fig. 14. $\mathrm{E_b}/\mathrm{N_0}$ at $\mathrm{BER} = 10^{-3}$ versus different values of the bursts' interarrival time for all of the examined coding schemes and the proposed impulsive noise model.

In Fig. 13, we observe that when the impulse burst duration increases, the system's performance drops, since greater $\mathrm{E_b}/\mathrm{N_0}$ values are necessary to achieve the same BER. This behavior is anticipated, provided that when the impulsive noise lasts longer, it damages more data blocks leading to greater errors at the receiver. Conversely, the results in Fig. 14 illustrate that for higher interarrival time values, we obtain enhanced performance. This is again in agreement with the theory, defining that the more often the noise bursts occur, the more data bits

TABLE IV
BER THRESHOLDS FOR E_B/N_o VALUES

E_b / N_0	BER threshold
2	0,37471
9	0,1563
14	0,031828
19	0,008915
24	0,0028598
29	0,00052238
34	0,00003646
37	0,000004083

will be harmed, resulting in poorer BERs. It is also noticeable from Figs. 13 and 14 that coding schemes requiring a lower modulation order experience better performance than the other coding techniques. GAC codes show greater tolerance to noise than RAC codes which comes in agreement with the results displayed in Figs. 7–12.

V. HYBRID CODING TECHNIQUE FOR THE TIME-VARYING PLC CHANNEL

In this section, we suggest an alternative coding method for the time-varying PLC channel which is being modeled by the proposed noise model. The concept of this noise model implies that noise bursts occur randomly in time and affect several consecutive data blocks depending on their duration, while leaving other data blocks unaffected. What we suggest is to use two different coding schemes at the same system: 1) for the undamaged data blocks and 2) the other one for the data blocks influenced by the impulsive noise. In this way, the data blocks which have suffered severe damage by the impulsive noise, are encoded by a strong coding scheme, thus being offered greater protection. On the other hand, the unaffected data blocks, which, by definition, do not require the same kind of protection, are encoded by a less effective coding technique, thus leading to better bandwidth exploitation. For this purpose, we use the (8, 4, 4) GAC and the (15, 8, 4) RAC code. As it is noticed from the previous section, the former coding scheme experiences better performance than the second one, however, implying QPSK modulation as opposed to 16PSK modulation. In this section, these two coding techniques are used to encode the affected and unaffected by the impulsive noise data blocks, respectively.

At this point, the problem is focused on how to determine which blocks suffer from the consequences of the impulsive noise. Baring in mind that the data blocks are transmitted continuously, all we need to do is to track the first block influenced by each noise burst. We start transmitting our data by using the (15, 8, 4) RAC coding scheme. For each block decoded at the receiver, the resulting BER is calculated. If this BER is found to be greater than a specific value threshold, it means that a noise burst has occurred. This information is transferred easily back at the transmitter, indicating that the (8, 4, 4) GAC coding technique should be used for a fixed number of subsequent data blocks. The threshold is different for each E_b/N_0 value and can be specified by simulating the same system with the (15, 8, 4) RAC code, excluding the presence of the impulsive noise. Table IV shows the thresholds used for eight different E_b/N_0 values.

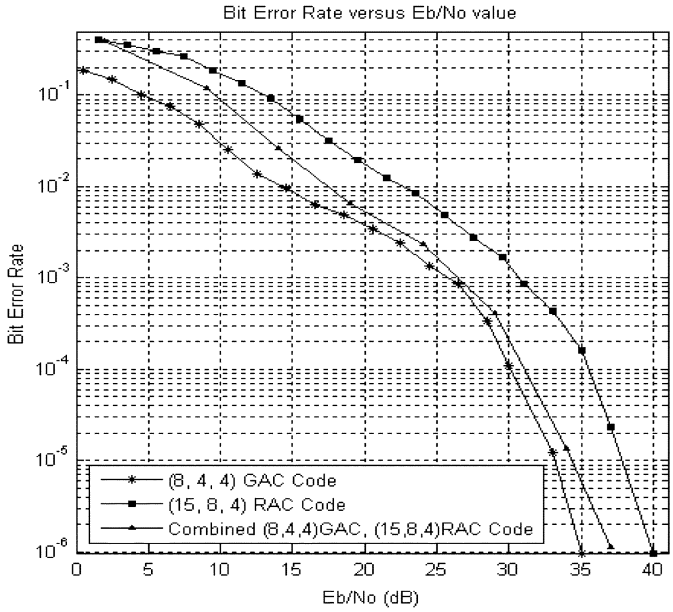

Fig. 15. BER versus E_b/N_0 by using the (8, 4, 4) GAC and the (15, 8, 4) RAC codes for the proposed impulsive noise model.

The fixed number of data blocks for which the (8, 4, 4) coding scheme is used, can be specified by taking into account the defined noise burst duration ($t = 0.1$ ms), the OFDM symbol properties, and the total bandwidth the PLC channel occupies. In [3], we find that the Zimmermann's channel model occupies a bandwidth from 0.3 to 20 MHz. This results in a total bandwidth of 19.7 MHz. We have also defined that the OFDM symbol consists of 256 carriers, whereas a cyclic extension of 20% takes place. According to OFDM transmission theory, each carrier takes up a frequency spectrum of Δf Hz and the OFDM symbol lasts for T_S seconds without taking its cyclic extension into account with

$$\Delta f = \frac{19,7 \cdot 10^6}{256} = 76953\,125\ \text{Hz} \tag{13}$$

$$T_S = \Delta f^{-1} = 1\,29949 \cdot 10^{-5}\ \text{sec.} \tag{14}$$

Since there is a cyclic extension of 20%, this leads to a total OFDM symbol duration of T_{OFDM} seconds, with

$$T_{\text{OFDM}} = T_S/0,8 = 1\,6243655 \cdot 10^{-5}\ \text{sec.} \tag{15}$$

By bearing in mind the defined noise burst's duration, we come to the conclusion that the burst will roughly influence seven data blocks.

After detecting the first data block influenced by the impulsive noise, we define the next six data blocks to be coded by the (8, 4, 4) GAC code, assuming that they also suffer severe damage from the impulsive noise. Consequently, the (15, 8, 4) RAC code is used until another affected data block is identified. Fig. 15 illustrates the performance in terms of BER regarding the system described before compared to the results obtained when the two coding schemes are used separately for the system's realization, under the same channel conditions.

At this point, it should be mentioned that 2000 data blocks were used for the simulation. The fact that the two coding

schemes require different modulation techniques, necessitated careful operations concerning the number of bits per block used to derive the BER.

It is concluded from Fig. 15 that the suggested coding method shows enhanced performance as opposed to the (15, 8, 4) coding scheme, whereas it is inferior to the (8, 4, 4) GAC coding technique. This is anticipated,since the suggested method takes advantage of both coding schemes. It is remarkable that as the $\mathrm{E_b/N_0}$ value increases, the system's performance for the combined coding technique comes close to the one regarding the (8, 4, 4) coding scheme. The benefit is that we obtain better bandwidth exploitation without sacrificing the system's performance at an unacceptable level.

VI. Conclusion

In this study, the performance of GAC and RAC coding techniques in power-line communications is examined. They are simple coding schemes and by altering their parameters, we obtain different codes of this family, thus adjusting in a better way to our system's demands. The results show that they could be considered to be a candidate coding scheme in the hostile PLC environment. In addition, two of the examined coding schemes were combined in order to meet the requirements of the time-varying PLC channel. The results show that this method leads to satisfying the system's performance while exploiting, in the best possible way, the available frequency bandwidth.

In addition, we propose a new way of modeling the unpredictable impulsive noise by taking the noise bursts' properties into account. Furthermore, the model's parameters are flexible so as to reflect the impulsive traffic and the power-line channel noise's conditions in general.

Appendix

The decoding procedure defining the RAC codes constitutes six steps [17].

1) Define the number of states $\mathrm{N_s}$ in the trellis as $N_s = q^{k_2}$, with $\mathrm{k_2}$ as the number of columns in the code (here, $\mathrm{q} = 2$).
2) Define the number of columns in the trellis as $\mathrm{N_c} = \mathrm{k_1} + 2$ with $\mathrm{k_1}$ as the number of rows in the code.
3) Each state at depth p, with $0 \leq \mathrm{p} \leq (\mathrm{N_c} - 1)$ is characterized by a k_2 tuple q-ary vector
$$S^p(A) = S^p(a_1, a_2, \ldots, a_j, \ldots a_{k_2}) \tag{16}$$
where a_j is an element of GF(q) and $j = 1, \ldots k_2$.
4) The trellis diagram starts at depth $p = 0$ and finishes at $p = N_c - 1$, with $S^0(0_1 0_2 \cdots 0_{k_2})$ and $S^{k+1}(0_1, 0_2, \ldots 0_{k_2})$ states, respectively.
5) The trellis branches at each depth p are labeled by a k_1 tuple q-ary vector C_A^p, where C_A^p is determined by
$$C_A^p(B) = S^p(A) \oplus S^{p+1}(A) \tag{17}$$
where A and B are all possible k_2 tuple q-ary vectors, standing for the present (p) and the next $(p+1)$ states of the trellis.
6) Two values characterize each branch, representing the input $C_A^p(a_1 \cdots a_{k_2})$ and the output $D_A^p(a_1 a_2 \cdots a_{k_2+1})$ vector, respectively, with $a_{k_2+1} = \sum_{i=1}^{k_2} a_i$.

On the other hand, concerning GAC codes, their encoding process is defined by the subsequent method [19].

1) A binary array code $\mathrm{C_1}$ $(n,\ k,\ d_{\min})$ is created with $R_1 = (\mathrm{n_2}, k_2, d_2)$ row codes, single parity check rows, and columns, where d_2 denotes the greatest integer close to $d_2/2$. In case n_0 is a prime number, we choose $n = n_0 + 1$
$$C_1 = \left.\begin{bmatrix} R \\ R \\ R \\ R \end{bmatrix}\right\} n_1 \text{ rows.} \tag{18}$$
2) A binary $n_1 * n_2$ product code $C_2 = |\mathrm{PA}|$ is produced, where P is a binary $n_1 * k_2$ array with only parity check elements whereas A is a binary $n_1 * (n_2 - k_2)$ matrix, whose columns are repetition codes and the first row consists of $k' = n_2 - k_2$ information bits
$$C_2 = [P \quad A]\} n_1 \text{ rows.} \tag{19}$$
3) A third binary product code C_3 is manufactured in case there are more information bits available
$$C_3 = \left.\begin{bmatrix} 0 \\ B \end{bmatrix}\right\} n_1 \text{ rows.} \tag{20}$$
B is a repetition row code $(n_0, 1, d_0)$ with k_0 information bits.
4) The desired code C is developed by adding the three product codes
$$C = C_1 \oplus C_2 \oplus C_3. \tag{21}$$
5) The symbol placed in the n_1th row and n_2th column is deleted if $n = n_0 + 1$.

As far as their decoding is concerned, there are a lot of similarities as well as differences with RAC codes. The design of a trellis diagram is also essential and it is constructed via the next procedure [19].

1) Define the number of states N_s in the trellis as $N_s = 2^{\max(k_p)}$, and the number of columns in the trellis as $N_c = n_1 + 1$, with k_p being the number of information bits in the pth row and n_1 as the number of rows.
2) Each state at depth p, with $0 \leq p \leq (N_c - 1)$ is characterized by a k_p tuple binary vector
$$S^P(A) = S^P(a_1, a_2, \ldots, a_j, \ldots a_{\max(k_p)}) \tag{22}$$
where $a_j = 0, 1$.
3) The trellis diagram begins at depth $p = 0$ and finishes at $p = n_2$, with $S^0(00 \cdots 0)$ and $S^{n_2}(00 \cdots 0)$ states, respectively.
4) Two values distinguish the trellis branches at depth p, X^P, and C^P, corresponding to the vector of information bits in the pth row and the vector of coded bits for this row, respectively
$$C^p = X_1^p \cdot G^p + C_2^p \tag{23}$$
where X_1^1 and C_p^2 represent codewords from the pth row of the C_1 and C_2 code correspondingly, while G_p is the generator matrix for the pth row code.

5) Each state $S^P(A)$ relates to its connecting next states $S^{P+1}(A)$ via (24)

$$S^{p+1}(A) = S^p(A) + X^p \tag{24}$$

6) In case C_3 is created during the code's design, the diagram's final depth implies that all states are joined to the last state with two parallel branches.

REFERENCES

[1] C. Hensen and W. Schulz, "Time dependence of the channel characteristics of low voltage power-lines and its effects on hardware implementation," *AEU Int. J. Electron. Commun.*, vol. 54, no. 1, pp. 23–32, Feb. 2000.

[2] H. Philipps, "Modelling of powerline communication channels," in *Proc. IEEE ISPLC*, 1999, pp. 14–21.

[3] M. Zimmermann and C. Dostert, "A multipath model for the powerline channel," *IEEE Trans. Commun.*, vol. 50, no. 4, pp. 553–559, Apr. 2002.

[4] T. Banwell and S. Galli, "A novel approach to the modeling of the indoor power line channel Part I: Circuit analysis and companion model," *IEEE Trans. Power Del.*, vol. 20, no. 2, pt. 1, pp. 655–663, Apr. 2005.

[5] S. Galli and T. Banwell, "A novel approach to the modeling of the indoor power line channel-Part II: Transfer function and its properties," *IEEE Trans. Power Del.*, vol. 20, no. 3, pp. 1869–1878, Jul. 2005.

[6] Y. Xiaoxian, Z. Tao, Z. Baohui, H. Zonghong, C. Jian, and G. Zhiqiang, "Channel model and measurement methods for 10-kV medium-voltage power lines," *IEEE Trans. Power Del.*, vol. 22, no. 1, pp. 129–134, Jan. 2007.

[7] K. Y. See, P. L. So, A. Kamarul, and E. Gunawan, "Radio-frequency common-mode noise propagation model for power-line cable," *IEEE Trans. Power Del.*, vol. 20, no. 4, pp. 2443–2449, Oct. 2005.

[8] B. M. Hansen, J. R. Ovesen, and K. Kolle, "Characteristics measurements using TDR and modelling of the transmission channel," in *Proc. IEEE ISPLC*, 2007, pp. 319–323.

[9] O. G. Hooijen, "On the channel capacity of the residential power circuit used as a digital communications medium," *IEEE Commun. Lett.*, vol. 2, no. 10, pp. 267–268, Oct. 1998.

[10] A. G. Burr and D. M. W. Reed, "HF broadcasting interference on LV mains distribution networks," in *Proc. ISPLC*, 1998, pp. 253–262.

[11] D. Benyoucef, "A new statistical model of the noise power density spectrum for powerline communication," in *Proc. IEEE ISPLC*, 2003, pp. 136–141.

[12] D. Liu, E. Flint, B. Gaucher, and Y. Kwark, "Wide band AC power line characterization," *IEEE Trans. Consum. Electron.*, vol. 45, no. 4, pp. 1087–1097, Nov. 1999.

[13] L. T. Pang, P. L. So, E. Gunawan, S. Chen, T. T. Lie, and Y. L. Guan, "Characterization of power distribution lines for high-speed data transmission," presented at the Int. Conf. Power System Technology, Perth, Western Australia, 2000.

[14] Z. Tao, Y. Xiaoxian, Z. Baohui, N. H. Xu, F. Xiaoqun, L. Changxin, and X. Jiaotong, "Statistical analysis and modeling of noise on 10-kV medium-voltage power lines," *IEEE Trans. Power Del.*, vol. 22, no. 3, pp. 1433–1439, Jul. 2007.

[15] H. Meng, Y. L. Guan, and S. Chen, "Modeling and analysis of noise effects on broadband power-line communications," *IEEE Trans. Power Del.*, vol. 20, no. 2, pt. 1, pp. 630–637, Apr. 2005.

[16] D. Middleton, "Statistical-physical model of electromagnetic interference," *IEEE Trans. Electromagn. Compat.*, vol. EMC-19, no. 3, pp. 106–126, Aug. 1977.

[17] K. M. S. Soyjaudah, "GAC and RAC codes in embedded format, employing inner and outer codes and trellis decoding," in *Proc. IEEE ICPWC*, 1999, pp. 409–413.

[18] K. M. S. Soyjaudah and G. Ramsawock, "Adaptive linear block coded quadrature amplitude modulation for time varying channels," in *Proc. Int. Conf. Telecommunications*, Acapulco, Mexico, 2000.

[19] K. M. S. Soyjaudah, "MPSK modulation using GAC codes," *Res. J. Sci. Technol.-Univ. Mauritius*, vol. 3, pp. 50–67, 1999.

[20] D. Yuan, C. Gao, and L. Zhang, "GAC-based trellis decoding of block codes in rayleigh fading channel," in *Proc. IEEE Conf. Wireless Communications and Networking*, Sep. 2000, vol. 3, pp. 1449–1452.

[21] D. Yuan, C. Gao, L. Zhang, and Z. Cao, "Generalized array codes for wireless image communication in presence of fading," in *Proc. IEEE Conf. Communications*, 2001, vol. 2, pp. 408–411.

[22] H. Nakagawa, D. Umehara, S. Denno, and Y. Morihiro, "A decoding for low density parity check codes over impulsive noise channels," in *Proc. IEEE ISPLC*, 2005, pp. 85–89.

[23] G. Pay and M. Safak, "Performance of DMT systems under impulsive noise," in *Proc. IEEE ISPLC*, 2001, pp. 109–114.

Nikoleta Andreadou (S'04–M'05) was born in Komotini, Greece, in 1981. She received the B.Sc. degree in electrical and computer engineering from the Democritus University of Thrace, Thrace, Greece, in 2004, the M.Sc. degree in mobile communication systems from the University of Surrey, Surrey, U.K., in 2005, and is currently pursuing the Ph.D. degree in electrical and computer engineering at the Aristotle University of Thessaloniki, Thessaloniki, Greece.

Her current research interests include power-line communications, signal processing, coding, and modulation techniques.

Ms. Andreadou is a member of the Technical Chamber of Greece.

Fotini-Niovi Pavlidou (S'86–M'87–SM'00) received the Ph.D. degree in electrical engineering from the Aristotle University of Thessaloniki (AUTh), Thessaloniki, Greece, in 1988.

Currently, she is with the Department of Electrical and Computer Engineering at AUTh, teaching in the areas of mobile communications and telecommunications networks. Her research interests are in the field of mobile and personal communications, satellite communications, multiple-access systems, routing, and traffic flow in networks and QoS studies for multimedia applications over the Internet. She has published many papers in refereed journals and conferences.

Dr. Pavlidou has participatied in many national and international projects (Tempus, COST, Telematics, IST) and has chaired the European COST262 Action on "Spread Spectrum Systems and Techniques for Wired and wireless Communications." She was a member of the TPC in many IEEE/IEE conferences and she has organized/chaired some conferences, such as the "IST Mobile Summit2002," the 6th "International Symposium on Power Lines Communications-ISPLC2002," and the "International Conference on Communications-ICT1998." She is a permanent reviewer for many IEEE/IEE journals and has served as Guest Editor for special issues in many journals. She is currently chairing the joint IEEE VT&AES Chapter in Greece.